Supporting Material

Multiscale model of dynamic neuromodulation integrating neuropeptide induced signaling pathway activity with membrane electrophysiology

Hirenkumar K. Makadia[1,†], Warren D. Anderson[1,2,†], Dirk Fey[3,†], Thomas Sauter[4], James S. Schwaber[1,2], and Rajanikanth Vadigepalli[1,2,*]

[1]Daniel Baugh Institute for Functional Genomics and Computational Biology, Department of Pathology, Anatomy and Cell Biology, Sidney Kimmel Medical College, Thomas Jefferson University, Philadelphia, PA, USA
[2]Graduate program in Neuroscience, Thomas Jefferson University, Philadelphia, PA, USA
[3]Systems Biology Ireland, University College Dublin, Dublin, Ireland
[4]University of Luxembourg, Life Sciences Research Unit, Luxembourg, Luxembourg

[†]These authors contributed equally to this work.
[*]Correspondence: Rajanikanth.Vadigepalli@jefferson.edu.

S1 Material balance of cytosolic calcium

Intracellular Ca^{2+} levels in the model were modulated by calcium currents (I_{Ca_L} and I_{NaCa}), in addition to a capacitive Ca^{2+} entry to the ER, a membrane calcium pump, and Ca^{2+} buffering processes in the ER (Figure 2A). Excess Ca^{2+} in intracellular levels is transported to ER and stored in Ca^{2+} buffer, which is released by IP3R activation. The mass balance of intracellular (cytosolic) Ca^{2+} is given by

$$\frac{d[\mathrm{Ca^{2+}}_{\mathrm{cyt}}]}{dt} = \underbrace{\frac{I_{\mathrm{NaCa}} - I_{\mathrm{Ca_L}}}{z v_{\mathrm{cell}} F} - r_{\mathrm{Epump}}}_{\text{Extracellular}} + \underbrace{N \cdot [\mathrm{CaBuffer}]_{\mathrm{T}} \left(k_{\mathrm{ER}}^{\mathrm{Ca^{2+}}} \cdot [\mathrm{Ca^{2+}}_{\mathrm{cyt}}] \cdot (1 - [\mathrm{CaBuffer}]_{\mathrm{B}}) - k_{-\mathrm{ER}}^{\mathrm{Ca^{2+}}} \cdot [\mathrm{CaBuffer}]_{\mathrm{B}} \right)}_{\text{Endoplasmic Reticulum}} \tag{1}$$

where I_{NaCa} is the NCX current, I_{Ca_L} is the L-type calcium channel current , $z(=2)$ is valency of Ca^{2+} ion, F is the Faraday's constant, v_{cell} is the soma volume, r_{Epump} is the rate of Ca^{2+} transfer through extracellular pump, $N(=40)$ is the number of binding sites on CaBuffer, $[\mathrm{CaBuffer}]_T$ is the total concentration of Ca^{2+} buffer in ER , $[\mathrm{CaBuffer}]_B$ is the concentration of bounded Ca^{2+} buffer in ER, $k_{ER}^{Ca^{2+}}$ is the inward rate of Ca^{2+} flux to the ER, and $k_{-ER}^{Ca^{2+}}$ is the outward rate of Ca^{2+} flux from the ER.

S2 Electrophysiology model details

We modeled neurophysiology with an electrical circuit (Figure 1B) containing multiple ionic currents, balanced across the membrane as shown in eqs. (2) to (5)

$$C\frac{dV}{dt} = -\sum_i g_i(V)\,(V - E_i) \tag{2}$$

$$g_i(V) = \bar{g}_i \cdot m_i^{M_i}(V) \cdot h_i^{H_i}(V) \tag{3}$$

$$\tau_{m,i}\frac{dm_i}{dt} = m_{\infty,i} - m_i \ ; \qquad \tau_{h,i}\frac{dh_i}{dt} = h_{\infty,i} - h_i \tag{4}$$

$$m_{\infty,i} = \left(1 + \exp\left(-\frac{V - V_{1/2,m,i}}{k_{m,i}}\right)\right)^{-x} \quad ; \quad h_{\infty,i} = \left(1 + \exp\left(\frac{V - V_{1/2,h,i}}{k_{h,i}}\right)\right)^{-x} \tag{5}$$

where C is the membrane capacitance; V is the voltage across the membrane; and for each ion channel i, g_i is the conductance, E_i is the reversal potential, $\bar{g}_i$ is the maximal conductance, m_i is the activation variable, h_i is the inactivation variable, and M_i and H_i are suitable parameters that are dependent on the kinetics of the channel activation/inactivation.

The time-varying membrane potential-dependent functions $m_i(V)$, $h_i(V)$ in eq. (4) are typically described using nonlinear functions (e.g., $m_{\infty_i} = f(V)$) depending on the paramterized form of Boltzmann functions characterized by half-activation voltage, $V_{1/2}$ and activation curve slope factor, k.

For channels characterized by the Hodgkin-Huxley formalism, the gating variable (p_i, analogous to m_i and h_i) is based on the probability of an individual gate being in a permissive state. Thus $(1 - p_i)$ is the probability of a non-permissive state. The transition between these states is described by first order kinetics:

$$\frac{dp_i}{dt} = \alpha_i(V)(1 - p_i) - \beta_i(V)p_i \tag{6}$$

in which α_i and β_i are voltage-dependent rate constants describing the "non-permissive to permissive" and "permissive to non-permissive" transition rates, respectively. The time course for approaching the equilibrium value of the gating variable (p_{∞_i}) can be described by a τ_i term. The resulting expressions used for solving eq. (6) are:

$$p_{\infty,i} = \frac{\alpha_i(V)}{\alpha_i(V) + \beta_i(V)} \qquad \tau_{p,i} = \frac{1}{\alpha_i(V) + \beta_i(V)} \tag{7}$$

In our modified model, K_{DR} activation was represented by a fourth order Boltzmann function ($x = 4$ in eq. (5)) based on experimental data from rat brain thalamic relay neurons [1]. The half activation voltage was set to 2.3 mV based on voltage-clamp data from brainstem neurons [2]. Our electrophysiology model was simulated as a single compartment (Figure 1B) with the following properties [3]: cell area = 0.0025 mm^2, membrane capacitance $C_m = 1$ uF/cm^2, and E_{leak} was set to maintain baseline firing rates at approximately 1.1 Hz in all simulations.

S3 Calcium baseline-dependent dampening of electrophysiological responses to AngII

We found that the baseline firing rate was elevated in the high Ca^{2+} baseline state (Figure S2A). This finding is consistent with elevated levels of active PKC and CaMKII leading to increased levels of K_{DR} phosphorylation and coincident reduction in hyperpolarizing drive. The excitability response for the high Ca^{2+} baseline condition was smaller and slower than that of the low Ca^{2+} baseline response. However, the steady state firing rates ($t = 300$ s) for high and low Ca^{2+} states were nearly identical, indicating that AngII normalizes the firing rates of cells with divergent Ca^{2+} baseline levels. To determine the electrophysiological basis of the observed excitability differences, we first examined membrane potential traces before and after applying AngII (Figure S2B). Membrane potentials during inter-spike intervals were at approximately -50 mV for both Ca^{2+} baseline conditions. Action potential waveforms and thresholds were also similar for high and low Ca^{2+} baseline states, both before and after applying AngII (Figure S2C). These results suggest that subtle differences in ionic currents during inter-spike intervals account for the Ca^{2+} baseline-dependent differences in firing rates.

To assess the ionic contributions to the membrane potential during inter-spike intervals, we examined membrane potential and current waveforms mediated by Na^+, K_{DR}, and K_{AHP} channels during intervals between APs (K_A and Ca_L currents were omitted because these did not vary in our simulations) (Figure S2D). For the high Ca^{2+} baseline state, firing rates were faster but the membrane potential was more hyperpolarized between APs. The high Ca^{2+} baseline state showed reduced Na^+ and K_{DR} currents along with increased K_{AHP} current between APs, compared to the low Ca^{2+} baseline state. These results are consistent with increased excitability in the high Ca^{2+} baseline states associated with enhanced Na^+ recovery from inactivation (Figure S3). Following AngII application, excitability properties were nearly identical for the low and high Ca^{2+} baseline states. This suggests that AngII drives divergent Ca^{2+} baseline neuronal conditions to a comparable electrophysiological state.

Table S1: **List of signaling pathway models.**

No.	Signaling pathway models	Initial parameter Ref.
1	Gq pathway activation	[4–6]
2	PLCβ hydrolysis	[4]
3	IP3 3-kinase activation	[4]
4	I(145)P3 dephosphorylation	[4]
5	I(1345)P4 dephosphorylation	[4]
6	Multiple inositol polyphosphate phosphatase	[4]
7	Interactions between Inositol high polyphosphates	[4]
8	Dynamics of IP4 interactions	[4]
9	I(134)P3 dephosphorylation	[4]
10	Calcium regulation	[3, 4, 7–11]
11	Calcium binding to calmodulin	[4]
12	CaMKII activation	[4, 12]
13	Protein kinase C activation	[4, 7, 12, 13]

Table S2: **Calcium regulation model. A schematic of the model is shown in Figure 2A.**

Modulation	Reaction	Parameters	Ref.
Calcium transport to ER	$2\,Ca^{2+}_{cyt} + CaTransp \underset{k_b}{\overset{k_f}{\rightleftharpoons}} CaTransp{-}2Ca^{2+}$	$k_f = 3600\ \mu M^{-2}s^{-1};\ k_b = 144\ s^{-1}$	[4]
	$CaTransp{-}2Ca^{2+} \xrightarrow{k_f} CaTransp + 2Ca^{2+}_{seq}$	$k_f = 25\ s^{-1}$	
	$Ca^{2+}_{seq} + CaTransp \underset{k_b}{\overset{k_f}{\rightleftharpoons}} CaTransp + Ca^{2+}_{cyt}$	$k_f = 8\ s^{-1};\ k_b = 8\ s^{-1}$	
Calcium buffer	$5\,Ca^{2+}_{seq} + Cabuffer \underset{k_b}{\overset{k_f}{\rightleftharpoons}} Cabuffer{-}5Ca^{2+}$	$k_f = 0.000489\ \mu M^{-5}s^{-1};\ k_b = 1\ s^{-1}$	[4]
	$5\,Ca^{2+}_{seq} + Cabuffer{-}5Ca^{2+} \underset{k_b}{\overset{k_f}{\rightleftharpoons}} Cabuffer{-}10Ca^{2+}$	$k_f = 0.000489\ \mu M^{-5}s^{-1};\ k_b = 1\ s^{-1}$	
	$5\,Ca^{2+}_{seq} + Cabuffer{-}10Ca^{2+} \underset{k_b}{\overset{k_f}{\rightleftharpoons}} Cabuffer{-}15Ca^{2+}$	$k_f = 0.000489\ \mu M^{-5}s^{-1};\ k_b = 1\ s^{-1}$	
	$5\,Ca^{2+}_{seq} + Cabuffer{-}15Ca^{2+} \underset{k_b}{\overset{k_f}{\rightleftharpoons}} Cabuffer{-}20Ca^{2+}$	$k_f = 0.000489\ \mu M^{-5}s^{-1};\ k_b = 1\ s^{-1}$	
	$5\,Ca^{2+}_{seq} + Cabuffer{-}20Ca^{2+} \underset{k_b}{\overset{k_f}{\rightleftharpoons}} Cabuffer{-}25Ca^{2+}$	$k_f = 0.000489\ \mu M^{-5}s^{-1};\ k_b = 1\ s^{-1}$	
	$5\,Ca^{2+}_{seq} + Cabuffer{-}25Ca^{2+} \underset{k_b}{\overset{k_f}{\rightleftharpoons}} Cabuffer{-}30Ca^{2+}$	$k_f = 0.000489\ \mu M^{-5}s^{-1};\ k_b = 1\ s^{-1}$	
	$5\,Ca^{2+}_{seq} + Cabuffer{-}30Ca^{2+} \underset{k_b}{\overset{k_f}{\rightleftharpoons}} Cabuffer{-}35Ca^{2+}$	$k_f = 0.000489\ \mu M^{-5}s^{-1};\ k_b = 1\ s^{-1}$	
	$5\,Ca^{2+}_{seq} + Cabuffer{-}35Ca^{2+} \underset{k_b}{\overset{k_f}{\rightleftharpoons}} Cabuffer{-}40Ca^{2+}$	$k_f = 0.000489\ \mu M^{-5}s^{-1};\ k_b = 1\ s^{-1}$	
Capacitive calcium entry to ER	$Ca^{2+}_{seq} + Capacitive{-}Ca_{active} \underset{k_b}{\overset{k_f}{\rightleftharpoons}} Capacitive{-}Ca_{inactive}$	$k_f = 0.6912\ \#^{-1}s^{-1};\ k_b = 6.25\ s^{-1}$	[4]
Calcium extracellular pump	$Ca^{2+}_{cyt} + CaEpump \underset{k_b}{\overset{k_f}{\rightleftharpoons}} CaEpump{-}Ca^{2+}$	$k_f = 1800\ \mu M^{-1}s^{-1};\ k_b = 288\ s^{-1}$	[4]
	$CaEpump{-}Ca^{2+} \xrightarrow{k_f} Ca^{2+}_{ext}$	$k_f = 72\ s^{-1}$	
	$Ca^{2+}_{ext} + CaEpump_{leak} \underset{k_b}{\overset{k_f}{\rightleftharpoons}} CaEpump_{leak} + Ca^{2+}_{cyt}$	$k_f = 0.2\ s^{-1};\ k_b = 0.2\ s^{-1}$	
	$Ca^{2+}_{ext} + CapacitiveChannel \underset{k_b}{\overset{k_f}{\rightleftharpoons}} CapacitiveChannel + Ca^{2+}_{cyt}$	$k_f = 0.01\ s^{-1};\ k_b = 0.01\ s^{-1}$	
IP3R activation	$IP3R + 3\,IP3{-}145 \underset{k_b}{\overset{k_f}{\rightleftharpoons}} IP3R_{active}$	$k_f = 0.05\ \mu M^{-3}s^{-1};\ k_b = 1\ s^{-1}$	[4]
	$Ca^{2+}_{seq} + IP3R_{active} \underset{k_b}{\overset{k_f}{\rightleftharpoons}} IP3R_{active} + Ca^{2+}_{cyt}$	$k_f = 3125\ s^{-1};\ k_b = 3125\ s^{-1}$	
Sodium-calcium exchanger	$r_{NaCa} = r_o \cdot m_{GHK} \cdot m_{chemical}$		[8–11]
	$m_{chemical} = -\left(1 + \frac{K_{PKCmod}}{1+\exp\left(\frac{K_{PKC}-100[PKC]-3}{D_{PKC}}\right)}\right)\left(\frac{[Ca^{2+}_{cyt}]}{k_m + [Ca^{2+}_{cyt}]}\right)\left(\frac{[Ca^{2+}_{cyt}]}{NaCa_{act} + [Ca^{2+}_{cyt}]}\right)$		
	$m_{GHK} = -\frac{\left([Ca^{2+}_{ext}][Na^{+}_{cyt}]^3\exp(\gamma\zeta)\right) - \left([Ca^{2+}_{cyt}][Na^{+}_{ext}]^3\exp((\gamma-1)\zeta)\right)}{1 + D_{NaCa}\left([Ca^{2+}_{cyt}][Na^{+}_{ext}]^3 - [Ca^{2+}_{ext}][Na^{+}_{cyt}]^3\right)}$		

r_{NaCa} = total Ca^{2+} flux, r_o = nominal flux gradient, m_{GHK} = electro-chemical flux across NCX, and $m_{chemical}$ = chemical gradient
$K_{PKCmod} = 0.5$, $K_{PKC} = 10$, $D_{PKC} = 2$, $k_m = 2$, $NaCa_{act} = 0.2$
$\gamma = 0.5$, $\zeta = \frac{zV_mF}{RT}$, $z = 2$, $F = 96500$ C mol^{-1}, $T = 310$ K, $R = 8314$ J kg^{-1} mol$^{-1}K^{-1}$, $D_{NaCa} = 0.05$ nM^{-4}

cyt – cytosolic; seq – sequestered; ext – extracellular; and V_m – membrane potential

Table S3: **Equations for the voltage dependence and kinetic current for brainstem neurons.**

Current			Expression	Ref.
I_{Na}	$\bar{g}_{\mathrm{Na}} \cdot m_{\mathrm{Na}}^3 \cdot h_{\mathrm{Na}} \cdot (E_{\mathrm{Na}} - V)$	$m_{\infty \mathrm{Na}}$	$\frac{0.091 \cdot (V+38)/(1-\exp(-(V+38)/5))}{0.091 \cdot (V+38)/(1-\exp(-(V+38)/5)) + 0.062 \cdot (V+38)/(\exp((V+38)/5)-1)}$	[3]
		$\tau_{m\mathrm{Na}}$	$(1/(0.091 \cdot (V+38)))/(1-\exp(-(V+38)/5)) + 0.062 \cdot (V+38)/(\exp(V+38)/5)-1)$	
		$h_{\infty \mathrm{Na}}$	$\frac{0.016 \cdot \exp(-(V+55)/15)}{0.016 \cdot \exp(-(V+55)/15) + 2.07/(1+\exp(-(V-17)/21))}$	
		$\tau_{h\mathrm{Na}}$	$1/(0.016 \cdot \exp(-(V+55)/15)) + 2.07/(1+\exp(-(V-17)/21))$	
$I_{\mathrm{K_{DR}}}$	$\bar{g}_{\mathrm{K_{DR}}} \cdot m_{\mathrm{K_{DR}}}^4 \cdot (E_{\mathrm{K}} - V)$	$m_{\infty \mathrm{K_{DR}}}$	$(1+\exp((V_{12}-V)/k))^{-4}$	[1]
		$\tau_{m\mathrm{K_{DR}}}$	$\frac{1}{4} \cdot (1/(\exp((V-81)/25.6)) + \exp((-(V+132)/18)) + 9.9)$	
$I_{\mathrm{K_A}}$	$\bar{g}_{\mathrm{K_A}} \cdot 0.4 \cdot m_{\mathrm{K_A}}^4 \cdot h_{\mathrm{K_A}} \cdot (E_{\mathrm{K}} - V)$	$m_{\infty \mathrm{K_A}}$	$1/(1+\exp(V+36/20))$	[3]
		$\tau_{m\mathrm{K_A}}$	$1/(\exp(V+35.82)/19.69) + \exp(-(V+79.69)/12.7) + 0.37)$	
		$h_{\infty \mathrm{K_A}}$	$1/(1+\exp(V+78/6))$	
		$\tau_{h\mathrm{K_A}}$	$1/(\exp(V+46.05)/5) + \exp(-(V+238.4)/37.45))$ if $V < -63$, else $\tau_{hK_A} = 60.0$	
$I_{\mathrm{K_{AHP}}}$	$\bar{g}_{\mathrm{K_{AHP}}} \cdot m_{\mathrm{K_{AHP}}}^2 \cdot (E_{\mathrm{K}} - V)$	$m_{\infty \mathrm{K_{AHP}}}$	$\frac{1.25 \cdot 10^{-8} [\mathrm{Ca}_{\mathrm{cyt}}^{+2}]^2}{(1.25 \cdot 10^{-8} [\mathrm{Ca}_{\mathrm{cyt}}^{+2}]^2) + 2.5}$	[3, 8]
		$\tau_{m\mathrm{K_{AHP}}}$	$1000/((1.25 \cdot 10^{-8} [\mathrm{Ca}_{\mathrm{cyt}}^{+2}]^2) + 2.5)$	
$I_{\mathrm{Ca_L}}$	$\bar{g}_{\mathrm{Ca_L}} \cdot m_{\mathrm{Ca_L}}^2 \cdot (E_{\mathrm{Ca}} - V)$	$m_{\infty \mathrm{Ca_L}}$	$\frac{1.6/(\exp(-0.072 \cdot (V-5)))}{1.6/(\exp(-0.072 \cdot (V-5))) + (0.02 \cdot (V-1.31)/(\exp((V-1.31)/5.36)-1))}$	[3]
		$\tau_{m\mathrm{Ca_L}}$	$1/(1.6/(\exp(-0.072 \cdot (V-5))) + (0.02 \cdot (V-1.31)/(\exp((V-1.31)/5.36)-1)))$	
I_{leak}	$g_{\mathrm{leak}} \cdot (E_{\mathrm{leak}} - V)$	-		[3]

$$\frac{dV_m}{dt} = \frac{1}{C_m} \cdot (I_{\mathrm{Na}} + I_{\mathrm{K_{DR}}} + I_{\mathrm{K_A}} + I_{\mathrm{K_{AHP}}} + I_{\mathrm{Ca_L}} + I_{\mathrm{leak}})$$

Note that $\mathrm{Ca}_{\mathrm{cyt}}^{2+}$ used in this Table is different from the cytosolic Ca^{2+} in Table S2. See first subsection of the Results for details.
I_{Na} – Fast sodium current, $I_{\mathrm{K_{DR}}}$ – Delayed rectifier potassium current, $I_{\mathrm{K_A}}$ – Fast activating potassium current
$I_{\mathrm{K_{AHP}}}$ – Hyperpolarized calcium dependent potassium current, $I_{\mathrm{Ca_L}}$ – High threshold calcium current

Table S4: **Model of phosphorylation of ion-channels through intermediate kinetics.**

Reaction	Rates	Parameters
$\mathrm{K_U} + 4\,\mathrm{PKC} \underset{k_{dp,PKC}}{\overset{k_{p,PKC}}{\rightleftharpoons}} \mathrm{K_{PKC}} + 4\,\mathrm{PKC}$	$k_{p,PKC}[\mathrm{K_U}][\mathrm{PKC}]^4 - k_{dp,PKC}[\mathrm{K_{PKC}}]$	$k_{p,PKC} = 10$; $k_{dp,PKC} = 0.7312$
$\mathrm{K_U} + 4\,\mathrm{CaMKII} \underset{k_{dp,CaMKII}}{\overset{k_{p,CaMKII}}{\rightleftharpoons}} \mathrm{K_{CaMKII}} + 4\,\mathrm{CaMKII}$	$k_{p,CaMKII}[\mathrm{K_U}][\mathrm{CaMKII}]^4 - k_{dp,CaMKII}[\mathrm{K_{CaMKII}}]$	$k_{p,CaMKII} = 1$; $k_{dp,CaMKII} = 3.3215$
$\mathrm{K_{CaMKII}} + 4\,\mathrm{CaMKII} \underset{k_{dp,CaMKII}}{\overset{k_{p,CaMKII}}{\rightleftharpoons}} \mathrm{K_{PKC,CaMKII}} + 4\,\mathrm{CaMKII}$	$k_{p,CaMKII}[\mathrm{K_{PKC}}][\mathrm{CaMKII}]^4 - k_{dp,CaMKII}[\mathrm{K_{PKC,CaMKII}}]$	$k_{p,CaMKII} = 1$; $k_{dp,CaMKII} = 3.3215$
$\mathrm{K_{PKC}} + 4\,\mathrm{PKC} \underset{k_{dp,PKC}}{\overset{k_{p,PKC}}{\rightleftharpoons}} \mathrm{K_{PKC,CaMKII}} + 4\,\mathrm{PKC}$	$k_{p,PKC}[\mathrm{K_{CaMKII}}][\mathrm{PKC}]^4 - k_{dp,PKC}[\mathrm{K_{PKC,CaMKII}}]$	$k_{p,PKC} = 10$; $k_{dp,PKC} = 0.7312$

$\mathrm{K_U}$ – Unphosphorylated potassium ion-channels ($\mathrm{K_{DR}}$), $\mathrm{K_{PKC}}$, $\mathrm{K_{CaMKII}}$ and $\mathrm{K_{PKC,CaMKII}}$ – phosphorylated potassium ion-channels ($\mathrm{K_{DR}}$)

Table S5: **Hill function models of signaling responses to AngII. Peak and steady state responses were separately normalized and fitted as functions of AngII concentration. Value pairs refer to the peak parameter value followed by the steady state parameter value.**

	Low Ca^{2+}		High Ca^{2+}	
	$K_{0.5}$ (nM)	nH	$K_{0.5}$ (nM)	nH
PLC	4.8, 5.51	1.06, 1.21	4.2, 4.3	1.04, 1.04
IP3	11.1, 9.3	1.06, 1.11	9.9, 9.9	1.08, 1.08
PKC	3.4, 3.3	1.07, 1.37	3.8, 3.8	1.03, 1.03
CaMKII	12.6, 12.6	1.59, 1.59	2.4, 2.4	1.51, 1.52

Table S6: **Hill function models of excitability responses to AngII. Peak and steady state responses were separately normalized and fitted as functions of AngII concentration. Value pairs refer to the peak parameter value followed by the steady state parameter value.**

Phenotype	$K_{0.5}$ (nM)	nH
Wildtype	25.6, 26.4	1.55, 1.53
Blocking PKC site	7.8, 6.3	1.09, 1.24
Blocking CaMKII site	4.1, 4.3	1.16, 1.50

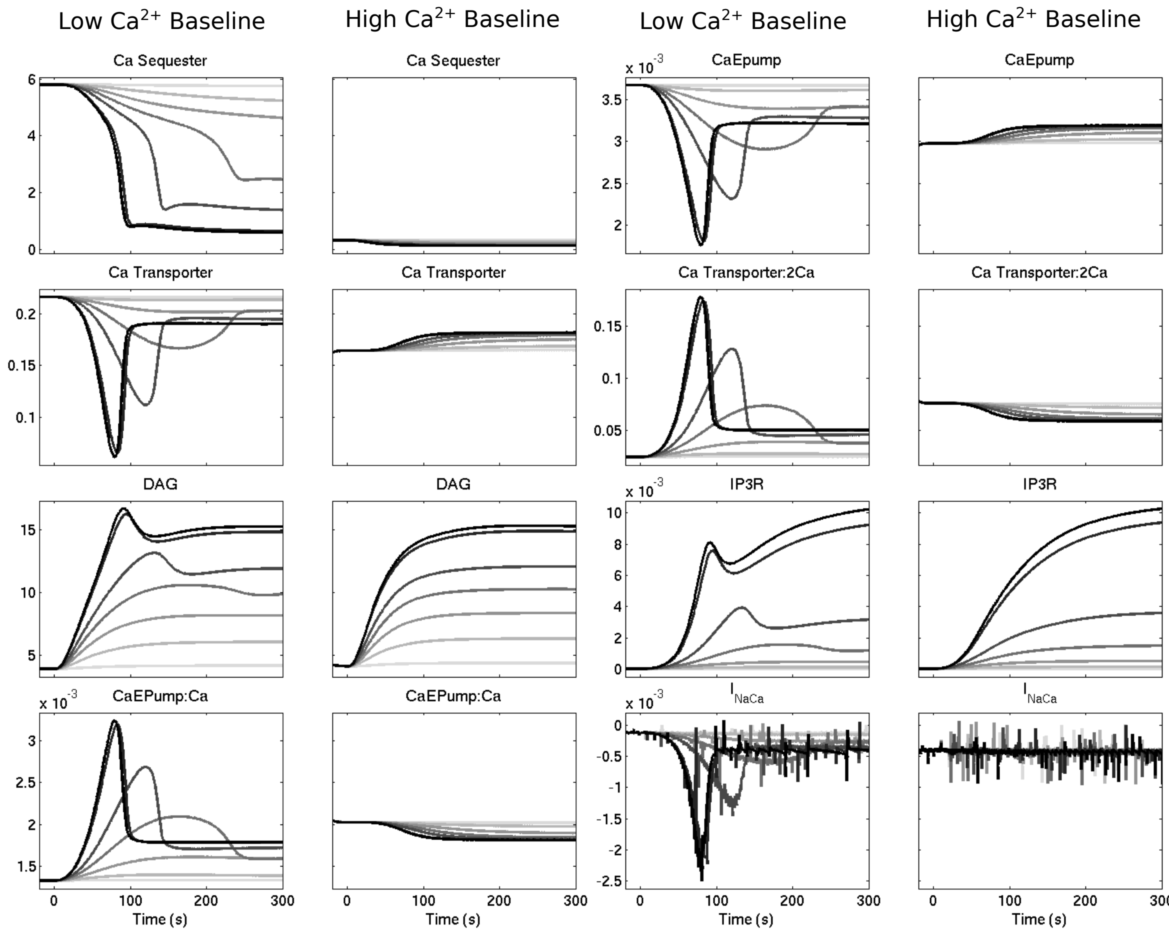

Figure S1: **Additional plots to Figure 2 of AngII elicited responses to different Ca^{2+} baseline conditions.** Low Ca^{2+} baseline and high Ca^{2+} baseline response plots to different doses of AngII for sequestered Ca^{2+}, CaTranp, DAG, CaEpump:Ca, CaEpump, CaTranp:2Ca, IP3R (IP3-bound IP3R) and NCX current (I_{NaCa}).

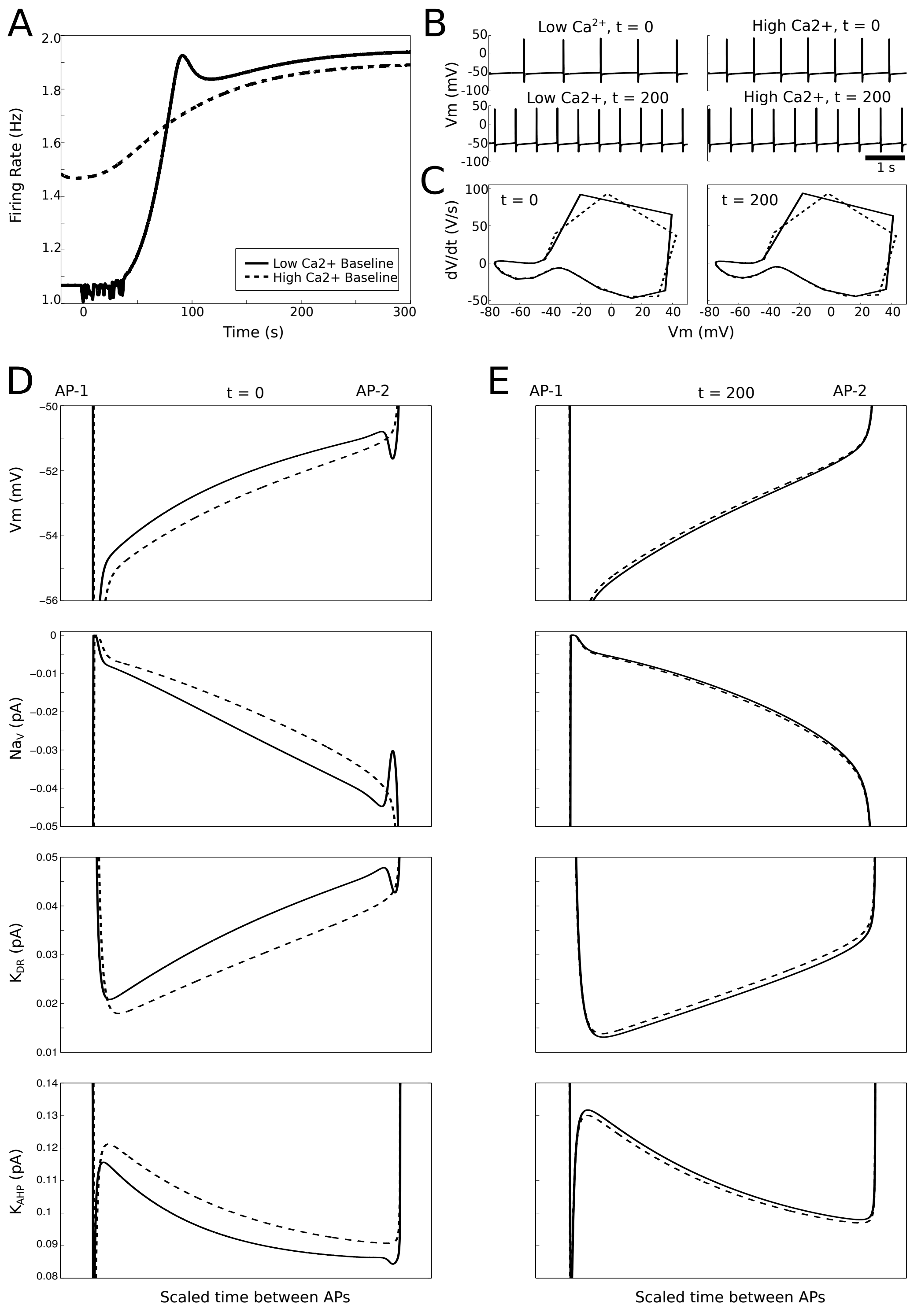

Figure S2: **Low Ca^{2+} baseline neuronal state exhibits a larger increase in AngII-induced excitability.** (A) Firing rate responses to AngII (100 nM at $t = 0$ s) are shown for low and high Ca^{2+} baseline levels. (B) Membrane potential waveforms are shown before ($t = 0$ s) and after ($t = 200$ s) AngII effects have stabilized. (C) Phase-space representations of APs before and after AngII (same legend as in panel A). (D) Biophysical differences between the low and high Ca^{2+} baseline conditions (same legend as in panel A). All data are plotted during normalized time intervals between two APs (AP-1 and AP-2) to show the inter-spike interval properties either before (left, $t = 0$ s) or after (right, $t = 200$ s) AngII stimulation. Abbreviations: Vm = membrane potential, Na_V = Na^+ current, K_{DR} = K_{DR} current, K_{AHP} = K_{AHP} current.

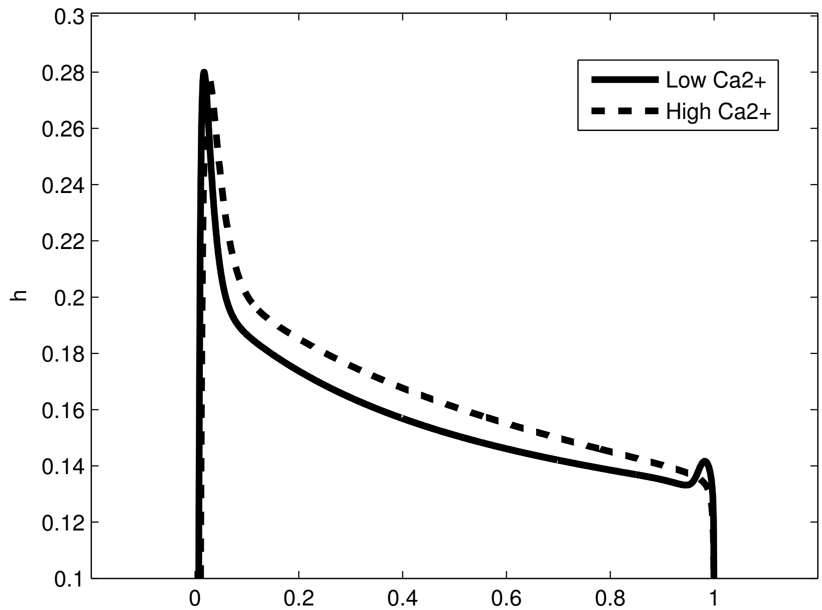

Figure S3: **Inactivation variable (h) for Na^+ channel at steady state for high and low Ca^{2+} baseline states.** Normalized time between two action potentials is represented as 0 to 1 on x–axis.

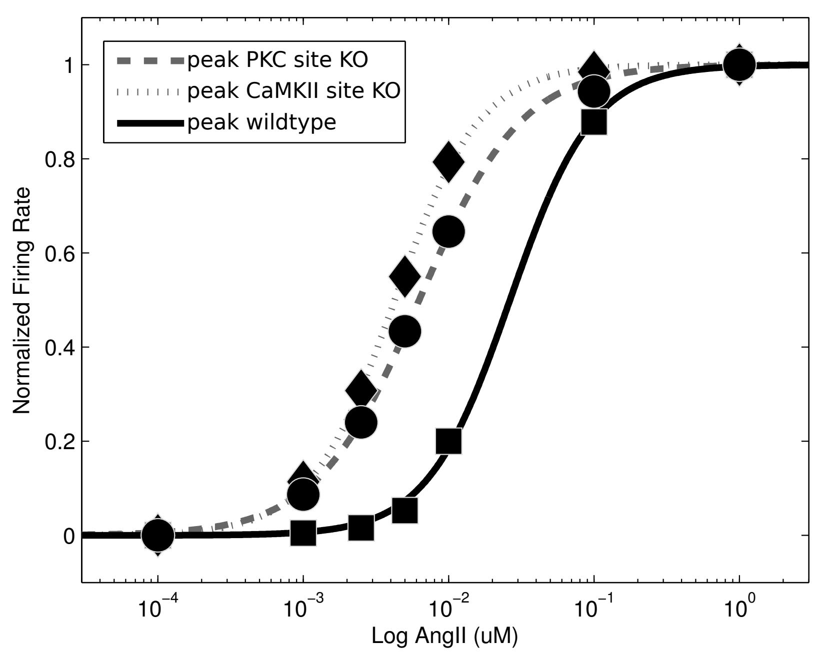

Figure S4: **Peak dose response curves for different blocking conditions of kinases.**

Supporting References

[1] J Huguenard and D Prince. Slow inactivation of a TEA-sensitive K current in acutely isolated rat thalamic relay neurons. *Journal of neurophysiology*, 66(4):1316–1328, 1991.

[2] C Gelband, J Warth, H Mason, M Zhu, J Moore, J Kenyon, B Horowitz, and C Sumners. Angiotensin II type 1 receptor-mediated inhibition of K+ channel subunit kv2.2 in brain stem and hypothalamic neurons. *Circulation research*, 84(3):352–359, 1999.

[3] I Rybak, J Paton, and J Schwaber. Modeling neural mechanisms for genesis of respiratory rhythm and pattern. i. models of respiratory neurons. *Journal of neurophysiology*, 77(4):1994–2006, 1997.

[4] J Mishra and U Bhalla. Simulations of inositol phosphate metabolism and its interaction with InsP3-Mediated calcium release. *Biophysical Journal*, 83(3):1298–1316, 2002.

[5] R Ouali, M Berthelon, M Bégeot, and J Saez. Angiotensin II receptor subtypes AT1 and AT2 are down-regulated by angiotensin II through AT1 receptor by different mechanisms. *Endocrinology*, 138(2):725–733, 1997.

[6] H Yang, D Lu, G Vinson, and M Raizada. Involvement of MAP kinase in angiotensin II-induced phosphorylation and intracellular targeting of neuronal AT1 receptors. *The Journal of Neuroscience*, 17(5):1660–1669, 1997.

[7] S Pan, M Zhu, M Raizada, C Sumners, and C Gelband. ANG II-mediated inhibition of neuronal delayed rectifier K+ current: role of protein kinase C-alpha. *American journal of physiology. Cell physiology*, 281(1):C17–23, 2001.

[8] A Athanasiades, Jr Clark, J, F Ghorbel, and A Bidani. An ionic current model for medullary respiratory neurons. *Journal of computational neuroscience*, 9(3):237–257, 2000.

[9] T Iwamoto, S Wakabayashi, and M Shigekawa. Growth factor-induced phosphorylation and activation of aortic smooth muscle Na+/Ca2+ exchanger. *The Journal of biological chemistry*, 270(15):8996–9001, 1995.

[10] T Iwamoto, T Watano, and M Shigekawa. A novel isothiourea derivative selectively inhibits the reverse mode of Na+/Ca2+ exchange in cells expressing NCX1. *Journal of Biological Chemistry*, 271(37):22391–22397, 1996.

[11] K Philipson, D Nicoll, M Ottolia, B Quednau, H Reuter, S John, and Z Qiu. The Na+/Ca2+ exchange molecule: an overview. *Annals of the New York Academy of Sciences*, 976:1–10, 2002.

[12] M Zhu, C Gelband, P Posner, and C Sumners. Angiotensin II decreases neuronal delayed rectifier potassium current: role of calcium/calmodulin-dependent protein kinase II. *Journal of neurophysiology*, 82(3):1560–1568, 1999.

[13] D Wang, C Sumners, P Posner, and C Gelband. A-type K+ current in neurons cultured from neonatal rat hypothalamus and brain stem: modulation by angiotensin II. *Journal of neurophysiology*, 78(2):1021–1029, 1997.